

# Electron spectra from autoionizing states of strontium and calcium excited by low- and intermediate-energy electrons

S.M. Kazakov and O. V. Khristoforov

*Chuvash State University, Cheboksary*

(Submitted 10 July 1984)

Zh. Eksp. Teor. Fiz. **88**, 1118–1130 (April 1985)

Ejected-electron spectroscopy was used to investigate the autoionizing states of strontium and calcium atoms. Resonant excitation of autoionizing states and their subsequent multichannel decay were recorded near threshold energies. The energy dependence of the intensities of a number of spectral lines is reported.

The autoionizing states (AIS) of strontium and calcium have frequently been investigated by photoabsorption methods. References to original publications can be found, for example, in Ref. 1. Most of this information refers to either very low-lying AIS, produced under the simultaneous excitation of both valence  $ns^2$  electrons, or states with excitation energy in excess of 100 eV, which are due to the excitation of the  $(n-2)p^6$  subshell or the simultaneous excitation of  $(n-2)d^{10}$  and  $(n-1)p^6$  electrons.

Studies of the electron spectra emitted by atoms as a result of the decay of the above autoionizing states have encountered considerable experimental difficulties, so that most investigations performed by ejected-electron spectroscopy have been confined to ejected-electron energies in the range  $E_{ej} = 10\text{--}30$  eV and have thus substantially added to existing information on the structure of autoionizing states. The trend in studies of AIS electron spectra has been gradually to reduce the collision energy and approach quite closely the thresholds of the autoionizing states.

The first measurements performed by ejected-electron spectroscopy involved the use of a 2-keV electron beam.<sup>2</sup> Schmitz *et al.* found 34 lines in the strontium spectrum and 22 lines in the calcium spectrum. They determined the excitation energies of atomic  $(n-1)p^5(n-1)dns^2\ ^1P_1$  levels and ionic  $(n-1)p^5ns^2\ ^2P_{1/2, 3/2}$  levels. We note that optically allowed transitions have the highest probability at such high collision energies.

The electron spectra of strontium were investigated in Ref. 3 at the lower energies of 70–1500 eV. A multichannel character of the decay of autoionizing states was proposed, but no convincing evidence for this was given. Calcium spectra obtained with the same spectrometer are discussed in Ref. 4. Analysis of observed lines and the variation in their intensities in the range 34–1500 eV have led to the conclusion that states that arise under one-electron excitation of the  $3p^3$ -subshell decay along a single channel with the formation of the CaII ion in the ground state  $3p^64s\ ^2S_{1/2}$ . In addition, some of the lines are interpreted in Ref. 4 as a manifestation of the multichannel AIS decay and are due to two- or three-electron excitation of the atoms. The number of observed channels does not exceed two.

The most productive (as far as the number of recorded lines is concerned) investigations of the autoionizing states of

strontium and calcium were those performed by the Ross group.<sup>5,6</sup> They recorded a large number of lines (83 in Sr and 165 in Ca) and compared these results with photoabsorption data and the results of other authors. The minimum collision energies attained in these experiments were 23.5 and 30 eV for strontium and calcium, respectively. A fraction of the lines was interpreted in Refs. 5 and 6 as being due to optically forbidden transitions. As for the classification of observed transitions, only a small number of individual lines has been identified so far, and many lines can only be classified as atomic or ionic. A substantial fraction of the lines cannot even be classified in this way. This situation is due to the absence of reliable photoabsorption data in this energy interval and to a number of other factors.

In this paper, we report an experimental study and an analysis of electron spectra emitted by strontium and calcium atoms and ions after the decay of autoionizing states. The spectra were obtained with an electron spectrometer incorporating a  $\pi/\sqrt{2}$  electrostatic energy analyzer. Particular attention was devoted, as usual, to the region of low collision energies and to the extension of the limits of the observed spectra. Studies of the autoionizing states near the AIS thresholds yield their excitation energies and thus enable us reliably to identify the lines as atomic or ionic. Resonant excitation of the AIS is also interesting and we have found (see below) that it enables us not only to demonstrate reliably the multichannel character of AIS decay and identify the decay channels, but also to explain previously observed features of ionization cross sections and of the excitation of resonant ionic levels.

## APPARATUS

A detailed description of the apparatus used in this research will be found in our earlier publications.<sup>7,8</sup> The crucible containing a few grams of pure metal was heated to a temperature corresponding to saturated vapor pressure  $P < 10^{-3}$  Torr. The temperature of the cell, energy analyzer, and electron-optical system exceeded the temperature of the crucible by 20–40 °C to prevent condensation of the vapor on their surfaces. The electron channel multiplier, used as the electron detector, was held at 200 °C. The electrostatic energy analyzer recorded electrons emitted at 90° to the primary-electron beam and was adjusted to transmit electrons with

the fixed energy of 1.0–1.5 eV. The energy resolution of the analyzer was 0.05–0.06 eV and the pulse-counting rate was  $10^5 \text{ s}^{-1}$ . The primary beam current at 200 eV was about 50  $\mu\text{A}$ .

### CALIBRATION OF BEAM ENERGY

The precision of experimentally determined primary-electron beam energy is an important question in studies of electron spectra near the threshold, in measurements of the energy dependence of line intensities, and in determinations of AIS excitation energies. Existing methods for the absolute energy calibration of electron beams are based on the determination of the appearance potentials for either current or optical radiation in the collision zone. Another common approach is to use reference energies, i.e., resonances in the energy dependence of scattering cross sections or spectral-line excitation functions. The use of these methods with electron spectrometers involves additional experiments or modifications of the available instrument. We have determined the absolute energy of the exciting beam by a method that is both simple and obvious. Its essence will become clear from the diagrams reproduced below (see, for example, Fig. 2). At low collision energies, the electron spectra contain both lines due to ejected and scattered electrons. The numbered bars in Fig. 2 indicate the inelastically scattered lines. These lines are broader in our spectra because of the considerable width of the primary-beam distribution function ( $\sim 0.3 \text{ eV}$ ). The scattered-line energies decrease with decreasing primary-beam energy and, therefore, intersect from right to left the "fixed" ejected-electron spectrum (see Fig. 2). The known energies in the AIS spectrum can be used to determine with high precision the absolute energies of the scattered lines  $E_{\text{scat}}$ . The known energy loss, i.e., the excitation energy  $E_a$  of a particular state, can then be used to find the beam energy

as the sum  $E = E_{\text{scat}} + E_a$ . Clearly, it is best to use isolated lines free from blends in this method. The precision of the method increases considerably as the widths of the instrumental functions of the energy analyzer and electron gun are reduced. In our particular case, the uncertainty in the measured energy is less than  $\pm (0.05\text{--}0.06) \text{ eV}$  for measured energies in the range 20–30 eV. Our numerous experiments using different atoms have shown that the method is convenient, accurate, and capable of automatic calibration of the energy at the maximum of the distribution function.

### RESULTS AND DISCUSSION

#### Strontium

Figure 1 shows the electron spectrum emitted after the decay of autoionizing states of strontium excited by a 200-eV electron beam. Figure 2 shows the structure of the spectra in the interval  $E_{\text{ej}} = 8\text{--}20 \text{ eV}$ , recorded for exciting beam energies of 22.65–21.44 eV. The ordinate axes in Figs. 1 and 2 are different.

We have investigated the primary-beam energy interval between 500 eV and the thresholds for the appearance of lines in the spectrum, i.e., approximately 21 eV. Narrow lines were not observed in the electron spectra at lower energies. When the energy dependence of the line intensities was determined under constant experimental conditions, we obtained a series of spectra by varying the primary-beam energy with a step varying from a few eV to a few tenths of eV, depending on the beam energy. The largest number of spectra was recorded near the threshold energies.

The absolute energy scale for the spectra was calibrated relative to reference line 63 ( $E_{\text{ej}} = 19.56 \text{ eV}$ ), which corresponds to the decay of the atomic  $4p^5 4d 5s^2 \ ^1P_1$  state observed in photo-absorption spectra (see, for example, Ref. 5).

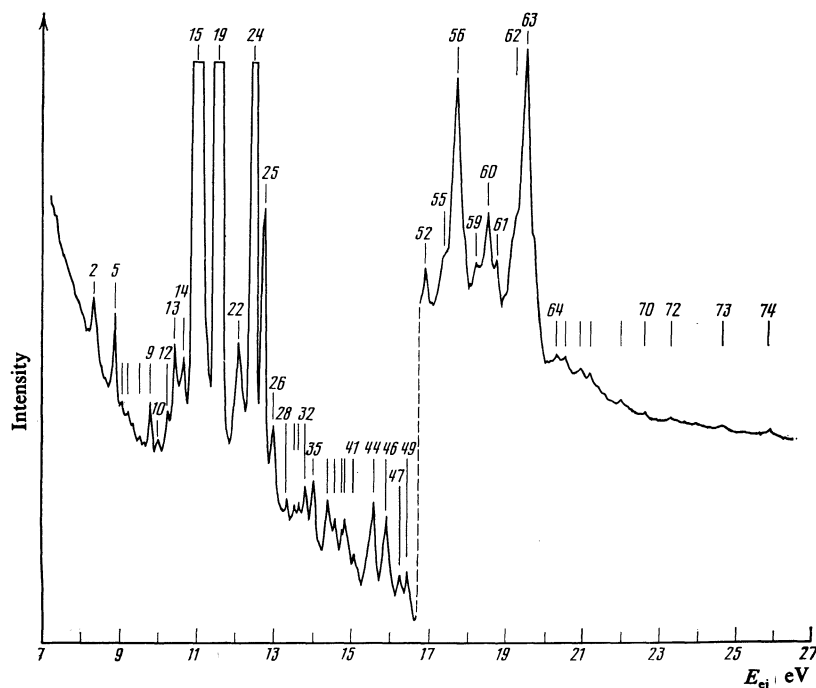


FIG. 1. Electron spectrum of strontium for beam energy  $E = 200 \text{ eV}$ .

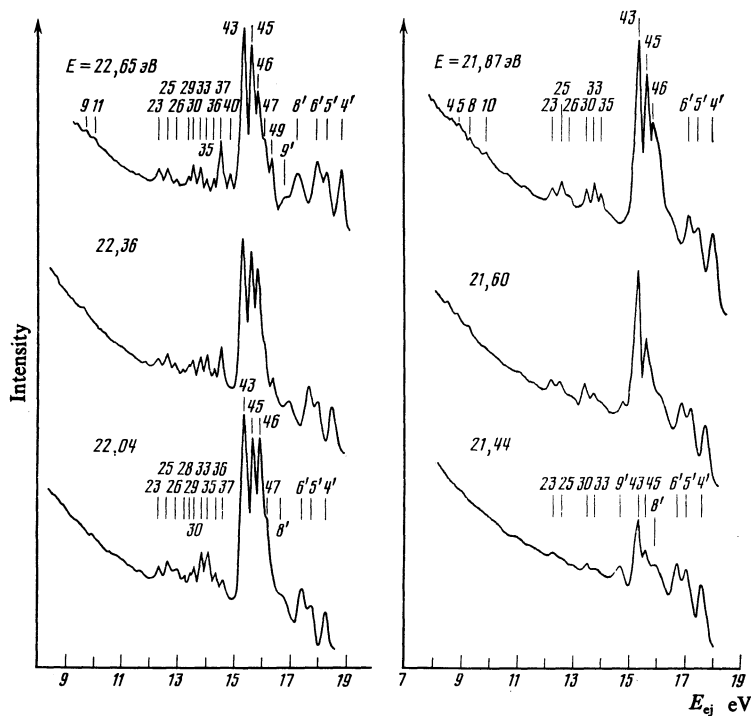


FIG. 2. Electron spectrum of strontium for threshold values of beam energy.

The linearity of the scale was checked in the course of the experiments against a number of other lines whose energies were known from previous work. For beam energies lower than the excitation energy of the above state, the reference line was line 43 ( $E_{ej} = 15.40$  eV), which is strong at low ener-

gies. The analogous line in the spectra obtained in Ref. 5 has  $E_{ej} = 15.43$  eV.

Table I lists the energies of the 74 lines that we have recorded in the ejected-electron energy range 7.9–25.8 eV. They are averages over many spectra. The energies of the

TABLE I.

Line No.	$E_{ej}$ , eV	Transition	Line No.	$E_{ej}$ , eV	Transition
1	7.94	Sr I (46) $\rightarrow 4p^6 7s^2 S_{1/2}$	38	14.57	Sr I (49) $\rightarrow 4p^6 4d^2 D_{3/2}$
2	8.22	—	39	14.81	Sr I (56) $\rightarrow 4p^6 5p^2 P_{1/2}$
3	8.49	Sr I (43) $\rightarrow 4p^6 6p^2 P_{1/2}$	40	14.89	Sr I (51) $\rightarrow 4p^6 4d^2 D_{3/2}$
4	8.61	Sr I (47) $\rightarrow 4p^6 4f^2 F_{5/2, 7/2}$	41	15.08	Sr I (52) $\rightarrow 4p^6 4d^2 D_{3/2}$
5	8.78	Sr I (43) $\rightarrow 4p^6 5d^2 D_{3/2}$	42	15.27	Sr I $\rightarrow 4p^6 5s^2 S_{1/2}$
6	8.94	Sr I (46) $\rightarrow 4p^6 6p^2 P_{3/2}$	43	15.40	Sr I $\rightarrow 4p^6 5s^2 S_{1/2}$
7	9.21	Sr I (47) $\rightarrow 4p^6 6p^2 P_{1/2}$	44	15.56	Sr I $\rightarrow 4p^6 5s^2 S_{1/2}$
8	9.37	Sr I (46) $\rightarrow 4p^6 5d^2 D_{3/2}$	45	15.69	Sr I $\rightarrow 4p^6 5s^2 S_{1/2}$
9	9.74	Sr I (45) $\rightarrow 4p^6 6s^2 S_{1/2}$	46	15.92	Sr I $\rightarrow 4p^6 5s^2 S_{1/2}$
10	9.90	—	47	16.12	Sr I $\rightarrow 4p^6 5s^2 S_{1/2}$
11	9.99	Sr I (46) $\rightarrow 4p^6 6s^2 S_{1/2}$	48	16.28	—
12	10.18	Sr II	49	16.38	Sr I $\rightarrow 4p^6 5s^2 S_{1/2}$
13	10.31	Sr II	50	16.46	Sr I $\rightarrow 4p^6 5s^2 S_{1/2}$
14	10.59	Sr II	51	16.79	Sr I $\rightarrow 4p^6 5s^2 S_{1/2}$
15	10.89	Sr II	52	16.85	Sr I $\rightarrow 4p^6 5s^2 S_{1/2}$
16	11.04	Sr II	53	17.06	—
17	11.21	Sr II	54	17.23	—
18	11.30	Sr II	55	17.37	Sr I $\rightarrow 4p^6 5s^2 S_{1/2}$
19	11.46	Sr II ( $4p^5 5s^2 2P_{3/2}$ )	56	17.69	Sr I $\rightarrow 4p^6 5s^2 S_{1/2}$
20	11.59	—	57	17.94	Sr I $\rightarrow 4p^6 5s^2 S_{1/2}$
21	11.80	Sr II	58	18.14	Sr I $\rightarrow 4p^6 5s^2 S_{1/2}$
22	12.03	—	59	18.27	Sr I $\rightarrow 4p^6 5s^2 S_{1/2}$
23	12.29	Sr I (43) $\rightarrow 4p^6 5p^2 P_{3/2}$	60	18.52	Sr I $\rightarrow 4p^6 5s^2 S_{1/2}$
24	12.40	Sr II ( $4p^5 5s^2 2P_{1/2}$ )	61	18.72	Sr I $\rightarrow 4p^6 5s^2 S_{1/2}$
25	12.64	Sr I (45) $\rightarrow 4p^6 5p^2 P_{3/2}$	62	19.17	Sr I $\rightarrow 4p^6 5s^2 S_{1/2}$
26	12.92	Sr I (46) $\rightarrow 4p^6 5p^2 P_{3/2}$	63	19.56	Sr I ( $4p^5 4d 5s^2 1P_1$ ) $\rightarrow 4p^6 5s^2 S_{1/2}$
27	13.10	Sr I (47) $\rightarrow 4p^6 5p^2 P_{3/2}$	64	20.30	Sr I $\rightarrow 4p^6 5s^2 S_{1/2}$
28	13.23	Sr I (47) $\rightarrow 4p^6 5p^2 P_{1/2}$	65	20.44	Sr I $\rightarrow 4p^6 5s^2 S_{1/2}$
29	13.44	Sr I (49) $\rightarrow 4p^6 5p^2 P_{1/2}$	66	20.83	Sr I $\rightarrow 4p^6 5s^2 S_{1/2}$
30	13.55	Sr I (43) $\rightarrow 4p^6 4d^2 D_{3/2}$	67	21.16	Sr I $\rightarrow 4p^6 5s^2 S_{1/2}$
31	13.66	Sr I (43) $\rightarrow 4p^6 4d^2 D_{3/2}$	68	21.93	—
32	13.74	—	69	22.08	—
33	13.82	Sr I (45) $\rightarrow 4p^6 4d^2 D_{3/2}$	70	22.57	—
34	14.00	—	71	22.84	—
35	14.06	Sr I (46) $\rightarrow 4p^6 4d^2 D_{3/2}$	72	23.25	—
36	14.32	Sr I (47) $\rightarrow 4p^6 4d^2 D_{3/2}$	73	24.58	—
37	14.52	Sr I (49) $\rightarrow 4p^6 4d^2 D_{3/2}$	74	25.81	—

strong lines were determined to within  $\pm 0.01$ – $0.02$  eV and the energies of the low-intensity lines to within  $\pm 0.03$ – $0.04$  eV. Comparable precision was probably achieved for lines measured against line 43 and observed at low collision energies. Our values of the line energy are in good agreement with Ref. 5.

Inspection of the ejected-electron spectrum ( $E_{ej} = 9$ – $17$  eV) recorded for primary-beam energies near the threshold values will show the presence of the strong lines 43–49 as well as a group of weaker lines at lower energies (see Fig. 2). If all these lines were due to the decay of atomic autoionizing states to the ground state of the singly charged ion, they should have been seen in our spectra down to energies  $E = E_{ej} + E_i$  and, as the beam energy was reduced, we should have observed the gradual disappearance of, first, the high-energy lines and then lines with lower energies. In fact, a different phenomenon was actually observed. The gradual vanishing of the lines was recorded only for the strong lines 43–49, for which the threshold energy was as calculated from the above formula, so that we could be sure that there were atomic autoionizing states with excitation energies of 21–22 eV. This is also confirmed by our observations of the strong line in the scattered-electron spectra with energy<sup>1)</sup>  $E_a = 21.4 \pm 0.1$  eV. We have not undertaken the identification of these lines, but it may be considered that they are due to the excitation of  $4p$  electrons.

The vanishing of the above lines from the spectrum was accompanied by the simultaneous vanishing of certain lines belonging to the low-intensity group as well, which suggested to us that the observed phenomena were due to a multichannel process. This could be seen in its purest form for beam energies below 22 eV (see Fig. 2). At  $E = 21.87$  eV, practically the only lines that remain from among the strong lines are lines 43, 45, and 46, but there are also two isolated groups, each of which consists again of only three lines. This suggests that each of the states 43, 45, and 46 decays into at least two excited states of SrII. Examination of the possible combinations of AIS excitation energies and the excitation energies of ionic levels has confirmed this hypothesis. The group of lines consisting of lines 23, 25, and 26 is shifted in energy relative to lines 43, 45, 46 by about 3 eV and the group 30, 33, 35 by 1.8 eV. The first of these groups is thus due to the decay of the atomic AIS 43, 45, 46 to the  $4p^6 5p^2 P_{1/2, 3/2}$ , state of SrII, and the second to the  $4p^6 4d^2 D_{3/2, 5/2}$  state of this ion. Lines corresponding to AIS decay to the excited states of the ion will be referred to as satellite lines. The assignment of satellite lines to particular atomic states is confirmed by the subsequent reduction in the energy of the pump beam (Fig. 2). The lower intensity of the principal line (transition to the ground state of the ion) leads to a reduction in the intensity of the corresponding satellite as well. The first to vanish from the spectra are the right-hand lines in all three groups, the intermediate lines vanish next, and the last to vanish is line 43 and its satellites (lines 23 and 30).

Another phenomenon may be responsible for the appearance of the satellites near the strong lines with energies  $E_{ej}$ . An electron emitted by an autoionizing may lose some of the energy  $E_a$  in an inelastic collision with a neutral atom as it passes through the electron-optics of the spectrometer,

which would lead to the appearance of a line with energy  $E_{ej} - E_a$ . It is natural to suppose that this will be accompanied by the excitation of the lowest-lying subthreshold levels of the atom, namely,  $5s5p^3 P_{012}$  with energies  $E_a = 1.77$ – $1.85$  eV. And since the excitation energies of the low-lying  $4p^6 4d^2 D_{3/2, 5/2}$  levels of SrII have roughly the same value (1.81 and 1.84 eV, Ref. 9), the two processes will be indistinguishable in the opinion of the authors of Ref. 5. We would agree with this conclusion, were we sure that the cross section for the excitation of the  $5s5p^3 P_{012}$  levels for incident electron energies  $E = 15$ – $17$  eV (the energy interval of the ejected electrons for lines 43–49) is much greater than the excitation cross sections for other subthreshold levels. It turns out that this is not the case. We have investigated the energy-loss spectra (the results will be published elsewhere) for electrons in strontium vapor for beam energies between the threshold for these processes and 30 eV. We found that, even for energies of 5–6 eV, the  $5s4d^3 D_{123}$ ,  $5s4d^1 D_2$ , and  $5s5p^1 P_1$  levels ( $E_a = 2.25$ – $2.69$  eV) have a much higher cross section, and the  $5s5p^1 P_1$  level is the most likely candidate. For  $E = 10^{15}$  eV or higher, the probability of excitation of the  $5s5p^3 P_{012}$  levels becomes negligible in comparison with the probability of excitation of the  $5s5p^1 P_1$  level. It follows that, if the process under consideration does, in fact, take place, one would expect the appearance of satellites with energies  $E_{ej} = 2.69$  eV, and these have not, in fact, been seen in our spectra at low beam energies. We may therefore conclude that multichannel autoionizing processes occur at a substantial rate in strontium atoms. The above analysis of the structure of the spectra and of line energies enabled us to identify a considerable proportion of the lines with multichannel transitions in the atoms (see Table I).

In addition, we have examined the energy dependence of many of the line intensities in the spectrum. Figure 3 gives the results for the above lines in the energy range 21–23 eV. This figure shows quite convincingly that lines due to the main transition and the satellite lines have only one threshold. As a rule, the satellite line intensity is much lower than that of the main lines (see Fig. 2). They are therefore shown on a somewhat increased scale in Fig. 3. However, we note that the decay of state 47 to the excited  $4p^6 4d^2 D_{3/2, 5/2}$  state of SrII (line 37) predominates over its transition to the ground  $4p^6 5s^2 S_{1/2}$  state.

The behavior of line 40 (see Fig. 2) is interesting. We suggest that it is due to the decay of an optically forbidden AIS to the ground state of SrII (Ref. 5). If this is the case, the line should be seen up to  $E \approx 20.6$  eV. However, it turns out that it vanishes from the spectrum for energies below 22.5 eV (see Fig. 2), which suggests that its true threshold lies above 20.6 eV. This means that it is a manifestation of the multichannel decay of some higher-lying state, namely, state 51 (see Table I).

The intensity maximum of lines that are the last to vanish from the spectrum is reached for energies of about 22 eV, which is probably an indication that  $Sr^-$  has resonant states in the immediate neighborhood of autoionizing states. The resonant character of AIS excitation near the threshold is more convincingly demonstrated by inspecting wider energy intervals (see Fig. 4). Line 43 has three maxima, i.e.,

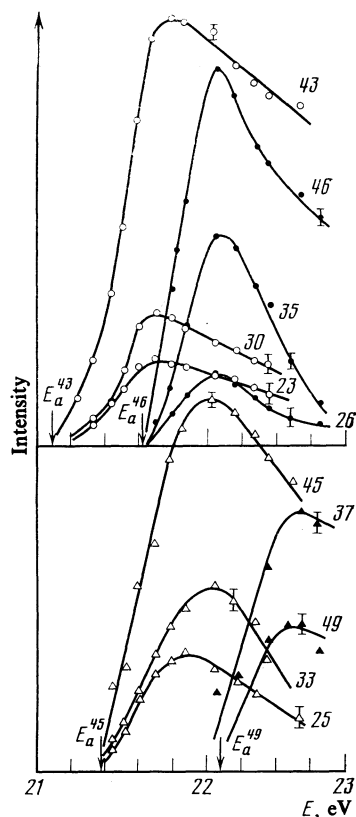


FIG. 3. Energy dependence of the intensity of several lines in the strontium spectrum near the threshold. The numeration of the curves is the same as in Table I.

$E_{\max} = 21.8, 25,$  and  $28$  eV. We identify the first of them with the resonant excitation of AIS 43 and the second (also narrow) may be either a resonant peak or a manifestation of the multichannel decay of higher-lying AIS with the formation of electron lines with energies close to  $E_{ej} = 15.40$  eV. In any event, the existence of resonances at  $E \approx 25$  eV demonstrates the energy dependence of the other measured lines.

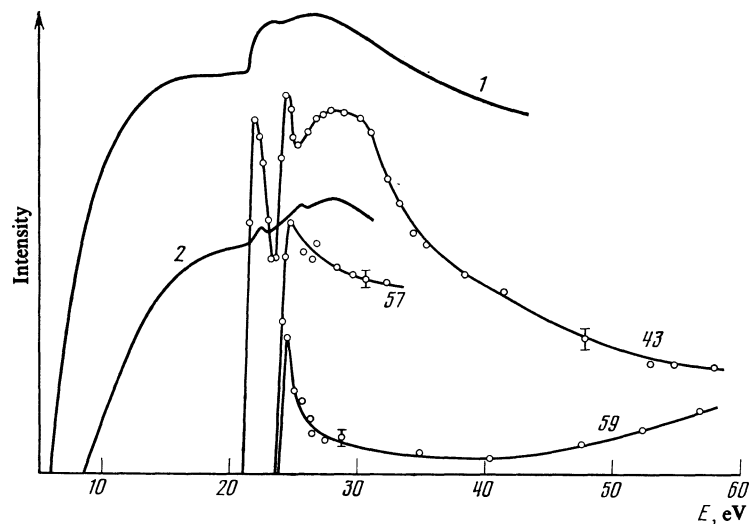
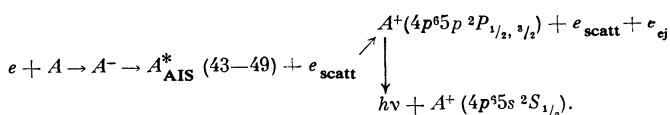


FIG. 4. Energy dependence of the intensities of lines 43, 57, and 59 of strontium. Curve 1—ionization cross section,<sup>10</sup> 2—excitation function of the resonance transition in the strontium ion.<sup>11</sup>

These are lines 57 and 59 (Fig. 4).

A broader maximum occurs at about 28 eV. Unusual breadth at  $\sim 30$  eV is also typical of other transitions (see Fig. 5). In addition to our own curves, Fig. 4 shows the energy dependence of the ionization cross section of the strontium atom<sup>10</sup> (curve 1) and the excitation function for the spectral line corresponding to the  $4p^65p^2P_{3/2} \rightarrow 4p^65s^2S_{1/2}$  resonant transition in strontium (curve 2) reported by the Gallagher group.<sup>11</sup> Both the ionization cross section and the line excitation cross section demonstrate the presence of a structure in the region 22-30 eV. It is clear from a comparison of our data with those reported by others that the above structure is due to autoionization processes occurring at a considerable rate in the region of the threshold energies, and to the particular type of decay of low-lying AIS in the  $4p$ -subshell, on the one hand, and multichannel AIS decay, on the other.

The irregularities on the line excitation function are responsible for the following processes:



We note that the structure of the excitation and the ionization cross sections is due to a combination of all the autoionizing transitions, so that a more rigorous and quantitative analysis of the reasons for the structural features could be made by summing the intensities of all the AIS at each energy or, better still, by summing the areas under all the autoionization resonances. In the case of the excitation function, this would require the summation of the areas under the resonances corresponding to transitions to the resonant  $4p^65p^2P_{1/2, 3/2}$  state of the ion SrII. Still better agreement would then be expected. However, we have not employed this method because of the unavoidable attendant errors. Nevertheless, the results that we have obtained provide a convincing explanation of the structure of the excitation and ionization curves.

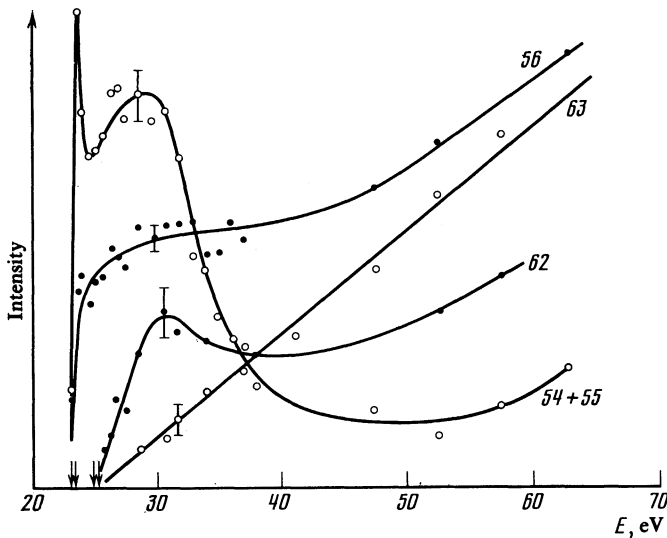


FIG. 5. Energy dependence of the intensities of lines 54, 55, 56, 62, and 63 in the strontium spectrum.

Figure 5 shows four different types of energy dependence of line intensity. The behavior of line 63 is particularly noticeable. This is the decay of the well-known optically allowed state of SrI ( $4p^5 4d 5s^2 1P_1$ ). As can be seen, there is a practically monotonic rise in intensity with energy, which explains the high line intensity at  $E = 200$  eV (see Fig. 1). Line 56 is also seen to have a growing intensity, which dominates the situation at high energies, but the line has a very diffuse maximum near the threshold. We note that different processes may contribute to the intensity of particular lines at different energies, and this is undoubtedly reflected in the behavior of intensity as a function of energy.

Line 62 ( $E_{ej} = 19.17$  eV) is a decay to the ground state of SrII of an autoionizing state with excitation energy  $E_a = 24.86$  eV. Aleksakhin *et al.*<sup>12</sup> have investigated the radiation spectra of autoionizing states in the vacuum ultraviolet, and have found the line at  $\lambda = 58.4$  nm. This line is emitted from a level with excitation energy  $E_a = 24.8$  eV (experimental threshold), which is very close to the excitation energy of line 62 in our spectra. Our experimental excitation function for the transition has a narrow peak at  $E = 30$  eV and a much broader maximum at  $E = 90$  eV. The decay curve for state 62 is also found to have a clear maximum at 30 eV, and the line intensity again increases for  $E > 40$  eV, i.e., there is a complete correlation between radiative and autoionization decay curves.

Finally, we draw attention to one further circumstance. When the beam energy approached the AIS threshold, we found a substantial broadening of the autoionizing resonances near lines 54–56, which might be due to post-collisional interaction between emitted and scattered electrons. Moreover, the multichannel decay of these states leads to the appearance of a still more broadened structure near lines 43–50, which takes the form of a bell-shaped distortion of underlying the continuous spectrum. For beam energies differing substantially from the excitation energies of lines 54–56, the background is monotonic in character. We may therefore

conclude that the structure of the AIS decay curves near the threshold may be due to both resonant and multiparticle processes.

### Calcium

Although, as indicated above, we have investigated the electron spectra for primary-beam energies in the range  $E_a < E < 500$  eV, here we shall confine our attention to lines recorded at  $E < 35$  eV. Figure 6 shows the electron spectrum at 35.38 eV. At this energy, the spectrum is quite complicated and consists of lines due to the decay of both atomic and ionic autoionizing states (see Table II). In addition, the spectrum contains lines *A*, *B*, *C*, and *D* due to scattered electrons. The energy loss corresponding to these lines is 24.87, 25.82, 27.11, and 27.48 eV, respectively. The decay of states with the given excitation energies leads to the appearance of the ejected-electron lines *A*-43; *B*-46, 47; *C*-50, 51; and *D*-52, 53. This spectrum thus contains lines characterizing both AIS excitation and AIS decay. We also observed higher-lying scattered-electron lines. In particular, energy was lost in the excitation of states 54–56 and others. We note that, between lines 43 and 46, 47 in the ejected-electron spectrum, there is the strong line 44, whilst there is not even an indication of its presence in the scattered-electron spectrum between lines *A* and *B*. This indicates that line 44 is not the decay of atomic AIS to the ground state of the singly-charged ion CaII.

A still more convincing confirmation of the multichannel nature of AIS decay is obtained by examining the spectra recorded for  $E < 30$  eV. A reduction in beam energy is accompanied by a reduction in the number of excited AIS, and the spectra become simpler (see Fig. 7). They no longer contain the ion lines, and consist of lines due to the multichannel decay of atomic AIS. The connection between lines due to the main transition and the corresponding satellite lines is demonstrated in Fig. 7, which shows in its upper part the level diagram of the ion CaII. This connection is even more firmly confirmed by considering the energy variation. As in the case of the strontium atoms, a change in the intensity of the main line is accompanied by a change in the intensity of its satellites, and they vanish simultaneously from the spectrum. Let us examine this for a number of transitions. At  $E = 27.16$  eV, the intensity of the line with the complex structure (line 46 + 47) is close to the maximum possible intensity. Its satellites, i.e., lines 33 and 39 (see Table II) attain maximum intensity at the same energy. Subsequent reduction in the beam energy is accompanied by a rapid reduction in the intensity of the lines, but other lines with lower energies show an increase in intensity. This refers, above all, to line 43, which consists of several closely spaced lines, one of which is the decay of a known optically-allowed state (see Table II). The rise in the intensity of line 43 is accompanied by an increase in the intensity of its satellites, i.e., the weaker lines 28 and 36. The final states for transitions 28 and 36 are the first excited states of CaII. The decay of AIS 43 to the higher-lying  $3p^6 5s^2 S_{1/2}$ ,  $3p^6 4d^2 D_{3/2, 5/2}$  and  $3p^6 5p^2 P_{1/2, 3/2}$  states of the ions also occurs at a considerable rate.

As expected, line 44 vanishes from the spectrum at energies greater than  $E = E_{ej} + E_i$ . Thus, it is already absent

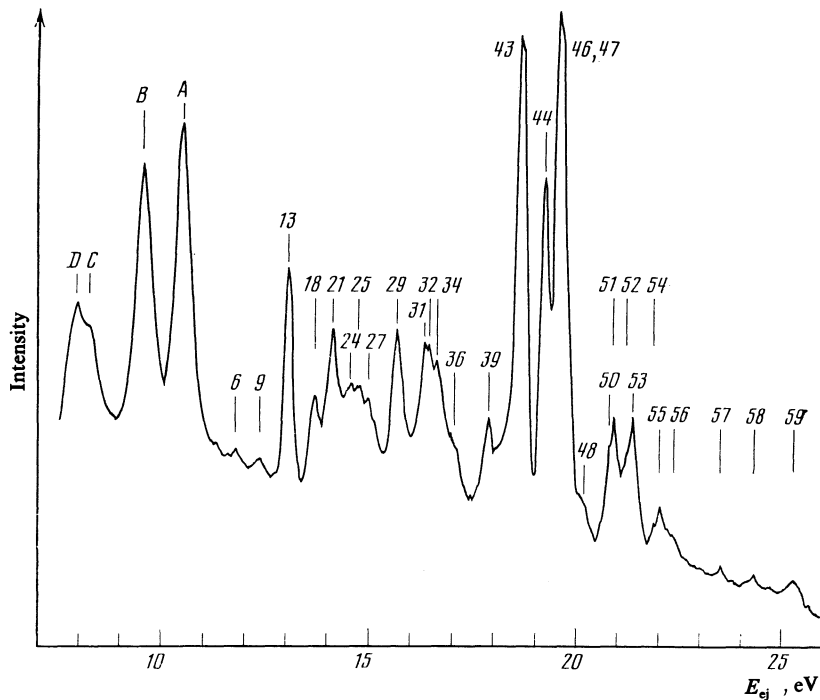


FIG. 6. Electron spectrum of calcium for beam energy of 35.38 eV.

at 26.15 eV (see Fig. 7), although it should have been observed up to 25.40 eV in the single-channel interpretation. There is no doubt that this line is the decay of state 50 ( $E_a = 26.92$  eV) to a metastable state of the ion CaII. The decay to the resonant state is also present in the spectrum, but is less well-defined. We note that decay to an excited

state occurs at a lower rate than that to the ground state.

Still more interesting is the behavior of the intensity of line 37 (see Fig. 7), which exhibits a clearly resonant behavior. The line appears only in a very narrow energy interval, and analysis shows that it is the decay of state 45 to the first excited  $3p^6 3d^2 D_{3/2, 5/2}$  state of CaII. The decay of state 45 to

TABLE II.

Line No.	$E_{ej}$ , eV	Transition	Line No.	$E_{ej}$ , eV	Transition
1	10.31	Ca I (43) $\rightarrow$ $3p^6 4f^2 F_{5/2, 7/2}$	30	16.30	Ca I (45) $\rightarrow$ $3p^6 4p^2 P_{1/2, 3/2}$
2	10.82	Ca I (46) $\rightarrow$ $3p^6 6s^2 S_{1/2}$	31	16.38	Ca II ( $3p^5 (3d^2 1S_0) 2P_{3/2}$ )
3	11.12	Ca I (46) $\rightarrow$ $3p^6 4f^2 F_{5/2, 7/2}$	32	16.47	Ca I (46) $\rightarrow$ $3p^6 4p^2 P_{1/2, 3/2}$
4	11.25	Ca I (43) $\rightarrow$ $3p^6 5p^2 P_{1/2, 3/2}$	33	16.62	Ca I (47) $\rightarrow$ $3p^6 4p^2 P_{1/2, 3/2}$
5	11.55	Ca I (50) $\rightarrow$ $3p^6 6p^2 P_{1/2, 3/2}$	34	16.70	Ca II ( $3p^5 (3d^2 1S_0) 2P_{1/2}$ )
6	11.72	Ca I (43) $\rightarrow$ $3p^6 4d^2 D_{3/2, 5/2}$	35	16.95	Ca I (48) $\rightarrow$ $3p^6 4p^2 P_{1/2, 3/2}$
7	12.17	Ca I (46) $\rightarrow$ $3p^6 5p^2 P_{1/2, 3/2}$	36	17.06	Ca I (43) $\rightarrow$ $3p^6 3d^2 D_{3/2, 5/2}$
8	12.26	Ca I (47) $\rightarrow$ $3p^6 5p^2 P_{1/2, 3/2}$	37	17.76	Ca I (45) $\rightarrow$ $3p^6 3d^2 D_{3/2, 5/2}$
9	12.31	Ca I (43) $\rightarrow$ $3p^6 5s^2 S_{1/2}$	38	17.85	Ca I (50) $\rightarrow$ $3p^6 4p^2 P_{1/2, 3/2}$
10	12.63	Ca I (46) $\rightarrow$ $3p^6 4d^2 D_{3/2, 5/2}$	39	17.92	Ca I (46) $\rightarrow$ $3p^6 3d^2 D_{3/2, 5/2}$
11	12.72	Ca I (47) $\rightarrow$ $3p^6 4d^2 D_{3/2, 5/2}$	40	18.10	Ca I (47) $\rightarrow$ $3p^6 3d^2 D_{3/2, 5/2}$
12	13.00	Ca II	41	18.30	Ca I (52) $\rightarrow$ $3p^6 4p^2 P_{1/2, 3/2}$
13	13.09	Ca II	42	18.36	Ca I (48) $\rightarrow$ $3p^6 3d^2 D_{3/2, 5/2}$
14	13.15	Ca I (46) $\rightarrow$ $3p^6 5s^2 S_{1/2}$	43	18.76	Ca I ( $3p^5 4s^2 3d^3 P_1$ ) $\rightarrow$ $3p^6 4s^2 S_{1/2}$
15	13.31	Ca I (47) $\rightarrow$ $3p^6 5s^2 S_{1/2}$	44	19.29	Ca I (50) $\rightarrow$ $3p^6 3d^2 D_{3/2, 5/2}$
16	13.50	Ca I (50) $\rightarrow$ $3p^6 5p^2 P_{1/2, 3/2}$	45	19.46	Ca I $\rightarrow$ $3p^6 4s^2 S_{1/2}$
17	13.56	Ca I (48) $\rightarrow$ $3p^6 5s^2 S_{1/2}$	46	19.62	Ca I $\rightarrow$ $3p^6 4s^2 S_{1/2}$
18	13.70	Ca II	47	19.77	Ca I $\rightarrow$ $3p^6 4s^2 S_{1/2}$
19	13.90	Ca I (50) $\rightarrow$ $3p^6 4d^2 D_{3/2, 5/2}$	48	20.10	Ca I $\rightarrow$ $3p^6 4s^2 S_{1/2}$
20	13.96	Ca I (52) $\rightarrow$ $3p^6 5p^2 P_{1/2, 3/2}$	49	20.33	Ca I (55) $\rightarrow$ $3p^6 3d^2 D_{3/2, 5/2}$
21	14.14	Ca II	50	20.81	Ca I $\rightarrow$ $3p^6 4s^2 S_{1/2}$
22	14.40	Ca I (52) $\rightarrow$ $3p^6 4d^2 D_{3/2, 5/2}$	51	20.97	Ca I $\rightarrow$ $3p^6 4s^2 S_{1/2}$
23	14.52	Ca I (50) $\rightarrow$ $3p^6 5s^2 S_{1/2}$	52	21.26	Ca I ( $3p^5 (3d^2 3P) 4s^3 P_1$ ) $\rightarrow$ $3p^6 4s^2 S_{1/2}$
24	14.56	Ca II	53	21.43	Ca I ( $3p^5 (3d^2 1D) 4s^3 P_1$ ) $\rightarrow$ $3p^6 4s^2 S_{1/2}$
25	14.77	Ca II	54	21.86	Ca II
26	14.96	Ca I (52) $\rightarrow$ $3p^6 5s^2 S_{1/2}$	55	22.03	Ca I $\rightarrow$ $3p^6 4s^2 S_{1/2}$
27	15.02	Ca II	56	22.35	Ca I $\rightarrow$ $3p^6 4s^2 S_{1/2}$
28	15.64	Ca I (43) $\rightarrow$ $3p^6 4p^2 P_{1/2, 3/2}$	57	23.50	Ca I $\rightarrow$ $3p^6 4s^2 S_{1/2}$
29	15.71	Ca II	58	24.30	Ca I $\rightarrow$ $3p^6 4s^2 S_{1/2}$
			59	25.25	Ca I ( $3p^5 4s^2 3d^1 P_1$ ) $\rightarrow$ $3p^6 4s^2 S_{1/2}$

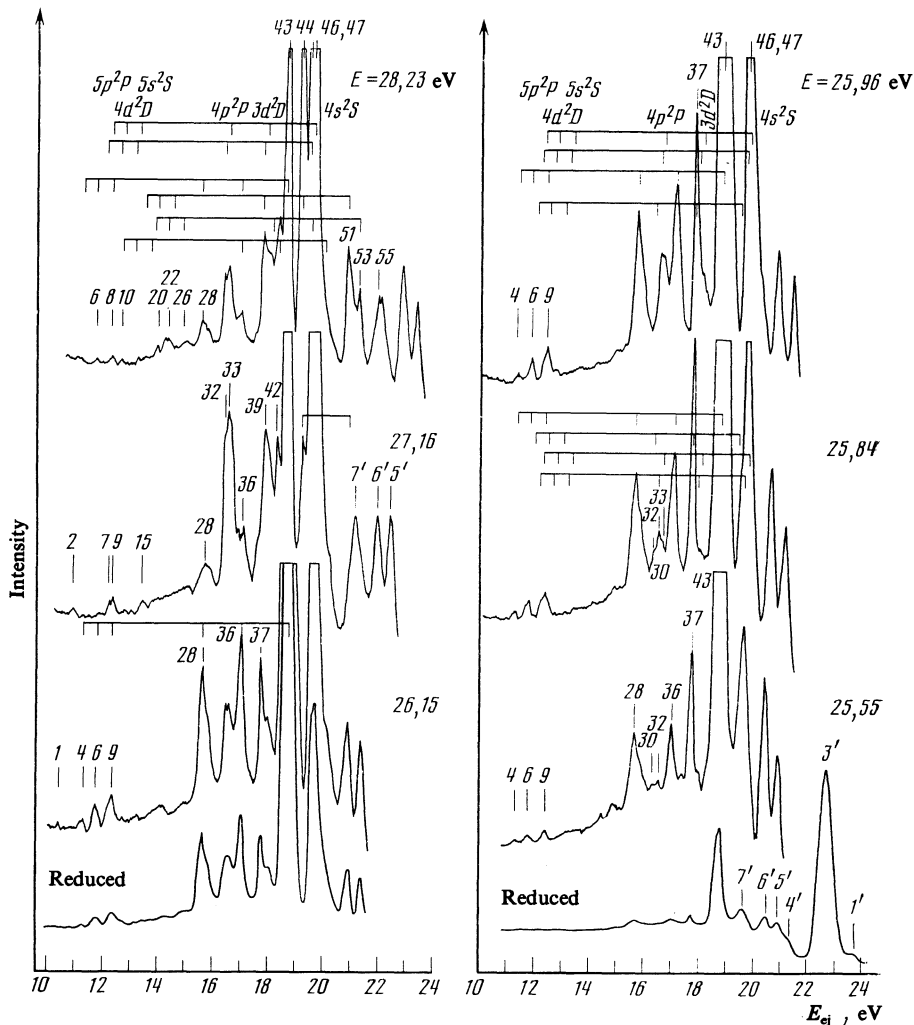


FIG. 7. Electron spectrum of calcium for threshold values of beam energy.

the ground state of the ion is not well-defined in the spectrum, and can be observed only at the energy of 25.84 eV against a background of lines 46 and 47 but, in this case, the decay to the excited state is predominant. Autoionization in calcium atoms is thus seen to lead to the substantial population of excited ionic states.

Figure 8 shows the energy dependence of the intensities of certain spectral lines. The decay curve for states 43 and 46, 47 have strong and narrow maxima near the threshold for the process, which we relate to the existence of short-lived states of negative ions  $\text{Ca}^-$  in the immediate neighborhood of the AIS thresholds, the decay of which leads to the effective population of atomic levels decaying as a result of autoionization. As expected, the energy dependence of satellite intensities is very similar to the curves for the main transition. For the sake of convenience in the determination of the relative line intensities, we show, against each curve in Fig. 8, the factor by which the ordinates have been multiplied as compared with the intensity of line 43. The figure also shows (curve 1) a portion of the energy dependence of the single-ionization cross section of the calcium atom.<sup>10</sup> As in the case of strontium, the behavior of the ionization curve is correlat-

ed with the behavior of the decay curve that we have recorded, i.e., the structure of the ionization function is due to the particular behavior of the excitation cross sections and the decay of the autoionizing states in the  $3p^6$  subshell. These processes also appear to be reflected in the excitation functions for the resonant transitions in CaII, but we have no information about them.

Figure 8 also shows the energy dependence of the intensity of line 37. There is a clear difference between the experimentally observed threshold for the appearance of the line and the threshold that follows from the single-channel interpretation. The transition is observed within an interval of only a few electron volts, and its width at half-height of maximum intensity does not exceed 0.4 eV. The character of the energy dependence suggests that the negative ions  $\text{Ca}^-$  play a leading role in the population of the decaying state, designated as state 45 in Table II. The resonant population and the dominating decay to the excited  $3p^6 3d^2 D_{3/2, 5/2}$  state of CaII make this an unusual AIS among the observed states.

The primed numbers in Fig. 7 mark the scattered electron lines in the spectrum. In particular, lines 1 and 3 correspond to the excitation of the  $4p^3 P_{012}$  and  $4p^1 P_1$  levels of the



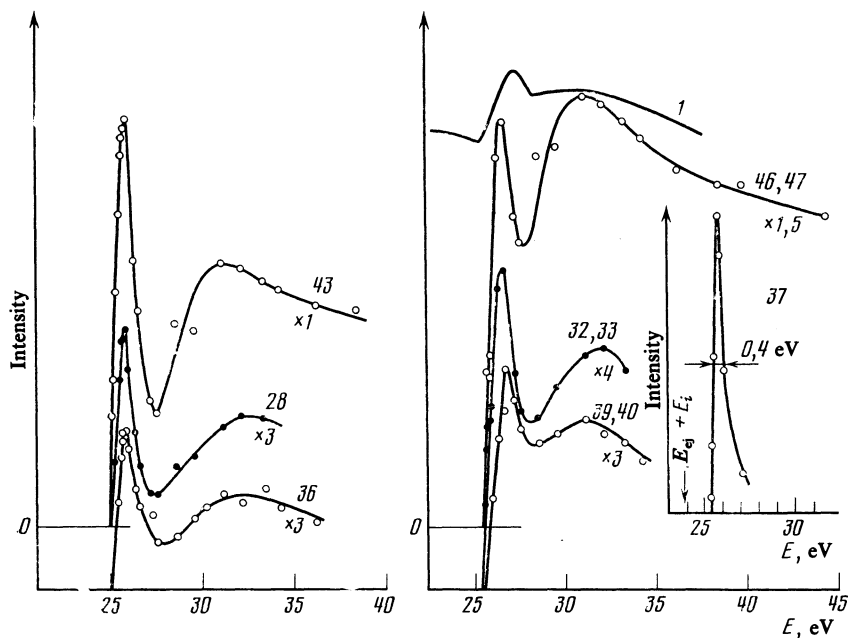


FIG. 8. Energy dependence of the intensities of certain lines in the calcium spectrum. The number shown against each curve corresponds to the line number in Table II. Curve 1 shows the ionization cross section of the calcium atom.<sup>10</sup>

atom. As in the case of strontium, the probability of excitation of the singlet level is much greater than the probability for the triplet level. The satellite lines in the ejected-electron spectra cannot, therefore, be explained by double collisions with the excitation of  $4p^3P_{012}$  levels.

### CONCLUSION

Our results show that strontium and calcium atoms have low-lying autoionizing states in the  $np^6$ -subshell, which are efficiently excited by electron impact. Near the threshold energies, most of the AIS are excited with the participation of short-lived states of the negative ions. As we have shown, the resonant contribution to the population of some of the AIS is very considerable, reaching factors of some tens or hundreds. The complex structure of the electron spectra of these elements is due to both the existence of optically forbidden states and appreciable multichannel processes. The number of observed decay channels is up to eight. We have detected states for which transitions to the excited states of the ion  $A^+$  predominate. All this has enabled us to provide a convincing interpretation of the features observed previously on the ionization curves and the excitation functions of ionic spectral lines.

<sup>10</sup>We also observed energy loss due to the excitation of higher-lying AIS with  $E_a = 23.4$  and  $25.3$  eV.

<sup>1</sup>M. G. Kozlov, *Spektry pogloshcheniya parov metallov v vakuumnom ultrafiolete* (Absorption Spectra of Metal Vapors in Vacuum Ultraviolet) [in Russian], Nauka, Moscow, 1981.

<sup>2</sup>W. Schmitz, R. Breuckmann, and W. Mehlhorn, *J. Phys. B. Atom. Mol. Phys.* **9**, L493 (1976).

<sup>3</sup>A. A. Borovik, *Ukr. Fiz. Zh.* **24**, 63 (1979).

<sup>4</sup>A. A. Borovik, I. S. Aleksakhin, and A. V. Kuplyauskene, *Opt. Spektrosk.* **51**, 433 (1981) [*Opt. Spectrosc. (USSR)* **51**, 239 (1981)].

<sup>5</sup>M. D. White, D. Rassi, and K. J. Ross, *J. Phys. B. Atom. Mol. Phys.* **12**, 315 (1979).

<sup>6</sup>V. Pejcev, T. W. Ottley, D. Rassi, and K. J. Ross, *J. Phys. B. Atom. Mol. Phys.* **11**, 531 (1978).

<sup>7</sup>S. M. Kazakov, A. I. Korotkov, and O. B. Shpenik, *Zh. Eksp. Teor. Fiz.* **78**, 1687 (1980) [*Sov. Phys. JETP* **51**, 847 (1980)].

<sup>8</sup>S. M. Kazakov and O. V. Khristoforov, *Zh. Eksp. Teor. Fiz.* **86**, 835 (1984) [*Sov. Phys. JETP* **59**, 488 (1984)].

<sup>9</sup>C. E. Moore, *Atomic Energy Levels*, CNBS 467, Washington, 1952, Vol. 2.

<sup>10</sup>S. Okudaira, *J. Phys. Soc. Jpn.* **29**, 409 (1970).

<sup>11</sup>S. T. Chen, D. Leep, and A. Gallagher, *Phys. Rev.* **13**, 947 (1976).

<sup>12</sup>I. S. Aleksakhin, G. G. Bogachev, I. P. Zaposochnyi, and S. Yu. Ugrin, *Dokl. Akad. Nauk USSR* **4**, 327 (1978).

Translated by S. Chomet